ROTATIONAL DISCONTINUITIES IN THE SOLAR WIND

by

James Marshall Turner

Center for Space Research
Massachusetts Institute of Technology
Cambridge, Massachusetts 02139

CSR-P-71-60

CENTER FOR SPACE RESEARCH
MASSACHUSETTS INSTITUTE OF TECHNOLOGY

Submitted to JGR May 1971

ROTATIONAL DISCONTINUITIES IN THE SOLAR WIND

by

James Marshall Turner

Center for Space Research
Massachusetts Institute of Technology
Cambridge, Massachusetts 02139

CSR-P-71-60

ABSTRACT

Solar wind plasma and magnetic field data from Mariner 5 are used to identify rotational discontinuities. Of the 40 discontinuities found, 36 were clustered in three distinct three to six day intervals. These three intervals were all characterized by high solar wind bulk velocities, high magnetic field magnitudes, low densities, and high correlation between velocity and magnetic field changes. This final characteristic along with the fact that the density and magnetic field magnitudes tended to be relatively steady provided strong evidence that smooth Alfven waves were also present during these times. The rotational discontinuities, which are sharp crested Alfven waves, had planes of polarization which were generally 10 - 20° away from the planes of polarization of the smooth Alfven waves previously mentioned. The planes of polarization of the rotational discontinuities were greatly different from the preferred orientation of tangential discontinuity surfaces which were found by the same spacecraft. An examination of the qualitative features of fast plasma streams and slow plasma streams revealed several striking differences in the behavior of the magnetic field and velocity and their fluctuations, the field magnitude, and the density. It is suggested that these differences are significantly correlated with the occurrence of rotational discontinuities.

Introduction

In this paper, solar wind plasma and magnetic field data from Mariner 5 are used to identify rotational discontinuities and Alfven waves in interplanetary space. The rotational discontinuities will be compared with Alfven waves and with tangential discontinuities found by the same spacecraft.

There was an earlier brief report by Turner and Siscoe (1971) which studied the same rotational discontinuities under consideration in this paper. However, this paper expands the original report to include also the comparison of rotational discontinuities with Alfven waves, examination of the characteristics of the solar wind away from the discontinuity and finally goes into more depth with regard to the state of the solar wind when the discontinuities were found.

There have been several papers which use the magnetohydrodynamic approximation to predict the properties of rotational discontinuities which are in fact large amplitude Alfven waves (see e.g. Colburn and Sonnett, 1966). Observations of Alfven waves were made by Coleman (1967) and Unti and Neugebauer (1968) from Mariner 2 data. More recently Belcher et al. (1969) have reported Alfven waves in Mariner 5 data.

In this paper as contrasted to the previous reports of Alfven waves particular attention will be focused on the rotational discontinuities and they will be examined as a subset of Alfven waves. As previously mentioned, the results will also be compared with tangential discontinuities. In the analysis done,

all three components of both the magnetic field and velocity were available.

The conclusions of this paper are that both rotational discontinuities and Alfven waves exist, with some differences in their polarizations. In addition, the rotational discontinuities have appreciably different planes of polarization from the orientation of the tangential discontinuity planes. Finally, the rotational discontinuities and Alfven waves were only found under certain conditions in the solar wind.

II. The Experiment

The Mariner 5 spacecraft was launched June 14, 1967 towards an encounter with Venus. The period of interest of this paper is the first forty days of the flight because the data acquisition rate was highest during this time.

A satellite centered RTN coordinate system was used: the R direction is radially outward from the sun, the T direction is parallel to the solar equatorial plane and positive in the direction of planetary motion, the N direction is directed northward along $\underline{R} \times \underline{T}$.

Magnetic field measurements were made by a low-field vector, helium magnetometer (Connor, 1968); three vector field readings were obtained every 12.6 seconds for the first forty days and every 50.4 seconds after that. The plasma detector, a modulated grid Faraday cup (Lazarus et al., 1967) pointed at the sun and measured positive ion currents in 32 energy levels from 40 to 9400 ev, with samples taken every 5.04 minutes at the high data rate.

The magnetic field data considered in the following analysis were 5.04 minute averages of the 12.6 second readings to make the magnetic field and plasma data comparable in time. The plasma parameters were obtained by fitting an isotropic Maxwellian distribution to the data. The uncertainties in the parameters are 10% in density, 1% in the radial component of the wind velocity, V_R, $\frac{\pi}{360}$ (i.e. $\frac{1}{2}^\circ$ in radians) x V_R for V_T, and V_N, and finally a few tenths of a gamma for the magnetic field components.

Selection of Rotational Discontinuities

The selection of rotational discontinuities was accomplished by a five step process. Three of the steps (numbers 1,4,5) are based on the properties of rotational discontinuities while two (numbers 2,3) are used primarily to insure reliable plasma and magnetic field parameters for the analysis.

The first step selected all times when $\underline{V}$ changed by 25 km/sec or more between consecutive measurements. This is based on the fact that in the plane of polarization of a rotational discontinuity $\underline{\Delta V} = \pm \underline{\Delta B} / \sqrt{4\pi\rho}$. If $\underline{\Delta B}$ is on the order of $\underline{B}$ then $\underline{\Delta V}$ is on the order of the Alfven speed. In the cases studied here, this condition is true. Since $V_A = 21.8\ B(\gamma)/\sqrt{n}$ (#/cc) where V_A is the Alfven speed in km/sec, B is the magnetic field in gammas, and n is the positive ion number density in particles per cm^3, it can be seen that for the usual solar wind conditions $V_A = 25$ km/sec would be lower than most measured Alfven speeds. Thus although it is not a necessary condition that $|\underline{\Delta V}| \geq 25$ km/sec, for most rotational discontinuities it can be expected that it is true.

The second step was taken to insure that the plasma and magnetic field parameters used later in the analysis were truly representative of the pre- and post-discontinuity solar wind. If a,b,c,d,e,f are consecutive data points with the velocity change of 25 km/sec or more occurring between points c and d, then it was required that the plasma and field parameters be relatively steady between points a,b, and c and similarly for points d,e, and f. By relatively

steady is meant that the parameters vary within a subjectively defined limit (generally 10%). This insures that the solar wind sample which was used to compute the values at b were entirely on one side of the discontinuity and similarly for point d. In later analysis, the pre-discontinuity solar wind state will be given by point b and the post-discontinuity state by point d.

The third step was taken to optimize the reliability of $\underline{B}_1 \times \underline{B}_2$ where $\underline{B}_1$ and $\underline{B}_2$ are the pre- and post-discontinuity magnetic fields respectively. This cross product is important because it is normal to the plane of polarization of a rotational discontinuity and the surface of a tangential discontinuity. If $\underline{B}_1$ and $\underline{B}_2$ are nearly parallel or anti-parallel, the cross product is not very reliable. The third step prevented this by imposing a limit on how close together $\underline{B}_1$ and $\underline{B}_2$ could be. Over the averaging period of $\underline{B}$, a standard deviation was computed for each component. Let σ_1 be the largest of the standard deviations for the components of the magnetic field at point b and let σ_2 be similarly defined for point d. Let $3\sigma/|\underline{B}|$ be the larger of $3\sigma_1/|\underline{B}_1|$ and $3\sigma_2/|\underline{B}_2|$. It was demanded that $\sin^{-1} 3\sigma/|\underline{B}| < \cos^{-1} (\underline{B}_1 \cdot \underline{B}_2/|\underline{B}_1|\ |\underline{B}_2|)$.

The fourth step was introduced to insure that the following two necessary conditions for a rotational discontinuity were satisfied: for an isotropic plasma, the density and magnitude of the magnetic field remain unchanged across the discontinuity. Thus it was required that the density and field magnitude change by no more than 10% which is on the order of the uncertainties in the two parameters. It should be noted that the field magnitude was measured separately from the field components. Occasionally, there would be a slight difference between the field magnitude and the square root of the sum of the

squares of the components.

The fifth and final step was taken to verify that another necessary condition for the rotational discontinuity not be violated. As mentioned previously in the plane of polarization the changed in $\underline{V}$ is either parallel or anti-parallel to the change in $\underline{B}$, i.e. $\underline{\Delta V} = \pm \underline{\Delta B}/\sqrt{4\pi\rho}$. However since the velocity and magnetic field normal to the plane remain unchanged across the discontinuity, the overall change in velocity must be parallel or anti-parallel to the overall change in $\underline{B}$. To satisfy this condition, it was required that $\left|\underline{\Delta V}\cdot\underline{\Delta B}/|\underline{\Delta V}||\underline{\Delta B}|\right| \geq 0.7$.

In all, there were 40 events which satisfied all the criteria. Data from a typical event are shown in Figure 1.

Matrix Technique

The major portion of the analysis of the data utilized a matrix technique for determining the distributions of sets of vectors in the rotational discontinuity data. Consider a set of N measurements of a vector $\underline{A}$. The real, sysmmetric matrix $T_{\ell m}=\sum_{k=1}^{N} A_{\ell}^{(k)} A_{m}^{(k)}$ can be formed where $A_{\ell}^{(k)}$ is the ℓth component of the kth vector. The three orthonormal eigenvectors of the matrix give an indication of the preferred directions of the set of vectors. The strength of the preferrence can be found by computing $\epsilon_i^2=\sum_{k=1}^{N}(\hat{A}^{(k)}\cdot\hat{e}_i)^2$, $(i=I, II, III)$ where $\hat{A}^{(k)}=\underline{A}^{(k)}/|\underline{A}^{(k)}|$ and $\hat{e}_i$ is one of the three eigenvectors. Thus an isotropic distribution would yield $\epsilon_I^2=\epsilon_{II}^2=\epsilon_{III}^2$. On the other extreme, if all the vectors were along the $\hat{e}_I$ direction, this distribution would make $\epsilon_I{}^2=N, \epsilon_{II}{}^2=\epsilon_{III}{}^2=0$.

It should be noted that in the discussion which follows ϵ_I will be associated with the eigenvector around which the $\underline{A}^{(k)}$ most tend to cluster, while ϵ_{III} will be associated with the eigenvector around which there is the least tendency to cluster.

Discussion of Results

1. Rotational Discontinuities

Of the 40 rotational discontinuities found, 36 occurred during three distinct three to six day time intervals. The first interval from decimal day 166 to 168 (group I) contained 13 events, the second from day 178 to 183 (group II) contained 16 events, and the third from day 193 to 197 (group III) contained 7 events. The solar wind had very similar qualitative characteristics during the three group intervals. In Figures 2, 3 and 4 are plotted the daily averages of V_R, $|\underline{B}|$, and n respectively and the three groups are indicated in the figures. Within each of the three groups, the bulk velocity has a relatively high value, the magnitude of the magnetic field also tends to be high while the number density is somewhat low. In addition, $|\underline{B}|$ and n are relatively steady during most of the time in each group. The four events which did not occur during any of the three groups were found on days 185, 186, 202, and 204 and a check of Figures 2 through 4 will show that these days were characterized by some but not necessarily all the qualitative features of the three groups. These qualitative features will be discussed in more detail later in the section dealing with comparison of fast and slow streams in the solar wind.

There were many similarities in the local characteristics of the discontinuities. In Figures 5 through 7 are shown polar plots of the change in the magnetic field across

the discontinuity for events in each of the three groups. In all cases $\Delta\underline{B}$ is taken to point outward, i.e. $\Delta B_R \geq 0$. In each figure, R is taken as the polar axis, so that the polar angle θ is measured outward from the center of the plot. The other angle, φ, is measured in the TN plane and is taken to increase clockwise away from the positive T direction toward the positive N direction. In all three groups φ tends to be in the vicinity of $\pm$ 90° for most cases, while θ is usually $\gtrsim$ 60°. A quantitative indication of these trends can be given by applying the matrix technique and the results for the three groups are presented in Table 1.

Table 1. - Eigenvectors for the Most Favored Direction of $\Delta\underline{B}$ Across a Rotational Discontinuity

	R	T	N	θ	ϕ	ε_i^2	ε_i^2/N	
$\hat{e}_I^{\Delta B_1}$	.582	.051	.812	54°	86°	6.805	.523	
$\hat{e}_{II}^{\Delta B_1}$	.726	.419	-.546	43°	308°	3.490	.268	(N=13)
$\hat{e}_{III}^{\Delta B_1}$	-.368	.907	.207	158°	13°	2.706	.208	
$\hat{e}_I^{\Delta B_2}$	.487	-.177	.855	61°	102°	9.158	.572	
$\hat{e}_{II}^{\Delta B_2}$	.618	.762	-.194	52°	346°	4.583	.286	(N=16)
$\hat{e}_{III}^{\Delta B_2}$	.617	-.623	-.480	52°	218°	2.592	.141	
$\hat{e}_I^{\Delta B_3}$	.770	.118	.627	40°	79°	4.614	.659	
$\hat{e}_{II}^{\Delta B_3}$	-.487	.743	.458	151°	32°	1.572	.224	(N=7)
$\hat{e}_{III}^{\Delta B_3}$	-.412	-.658	.630	156°	136°	0.815	.116	

Most of the changes in the direction of $\underline{B}$ across the discontinuity were relatively large with over 75% of the events having changes of 30° or more in the field direction. In addition since the changes were primarily in the RN plane, the plasma bulk speed was strongly affected since the velocity changes followed the field changes. Again in over 75% of the cases, V_R and thus the bulk speed changed by a significant amount which was typically 20 - 30 km/sec. Thus for the most part rotational discontinuities occurred within high velocity streams between relatively "fast" and "slow" moving plasma.

That $\Delta\underline{B}$ should have a substantial N-component is not surprising in view of the fact that known damping mechanisms of magnetic field fluctuations are not as strong out of the solar equatorial plane as they are within the solar equatorial plane (Belcher and Davis, 1970). The RT plane is only a few degrees away from the solar equatorial plane, so that fluctuations in the N-direction should in general be stronger. This was confirmed by Belcher and Davis (1970) using data from Mariner 5. However the strong preference for changes in B_R to accompany the changes in B_N may be a clue as to how the discontinuities are formed, since the B_R change must result in a V_R change.

2. Alfven Waves and Rotational Discontinuities

In addition to finding rotational discontinuities during the three groups, strong evidence presented in what follows also showed that Alfven waves were present for the duration of the group. This evidence of Alfven waves was not present at

other times. It was previously noted that the daily, as well as hourly, averages of n and $|\underline{B}|$ tend to be relatively steady within the three groups. Between the intervals of steady n and $|\underline{B}|$ there would be some change in both quantities on the time scale of an hour or two. Hence the three groups were dominated by these intervals of little or no change in n and $|\underline{B}|$ on the scale of one hour.

Further support for the claim that Alfven waves were present came from the very high correlation of changes in velocity and magnetic field during the three groups. The changes in the hourly averages of $\underline{V}$ and $\underline{B}$ were found from one hour to the next. The change in both quantities was normalized and the dot product of the normalized changes was computed. In Figure 8 is shown the percentage of cases for each day when this dot product is ≥ 0.90 in absolute value. Clearly the percentage is much higher during the group intervals. The cases of highest percentage also occur within one of the groups. A closer look at the dot product revealed that during the group intervals the dot product was consistently high for most or all of the day. Days not in the groups tended to fall into two catagories; the first being days when the dot product was low for most or all of the day, the second being days when the dot product was high for five or six consecutive hours and low the rest of the day. The latter category accounts for the days outside the groups when the percentage of dot products $\geq .90$ was high.

The result that the presence of Alfven waves was coincident with the presence of rotational discontinuities suggests strongly that the rotational discontinuities exist in a sea of smoother Alfven waves as opposed to the discontinuities existing in isolation from smoother Alfven waves.

The direction in which the Alfven waves fluctuate upon the background magnetic field may be found and this direction may be compared with the $\Delta\underline{B}$ across the discontinuities. To do this each day was divided into eight segments. The point-by-point changes in the magnetic field within each three hour segment containing a rotational discontinuity can be computed and a most likely direction of fluctuation found for that segment by the matrix technique. Then the most likely directions for the segments containing discontinuities during each group can be combined to yield a most likely direction of fluctuation for the Alfven waves near the set of discontinuities in the group. The only criterion for acceptability was that a segment had to contain at least half the maximum number of data points. The eigenvectors resulting from this for each group are presented in Table 2.

Table 2. - Eigenvectors for the Most likely Direction of Fluctuation in $\underline{B}$ for Segments Containing Rotational Discontinuities in Each Group

	$\underline{R}$	$\underline{T}$	$\underline{N}$	$\underline{\theta}$	$\underline{\phi}$	$\underline{\varepsilon_i^2}$	$\underline{\varepsilon_i^2/N}$	
$\hat{e}_I^{max}{}_1$	.365	.079	.928	69°	85°	5.161	.577	
$\hat{e}_{II}^{max}{}_1$	.750	.565	-.343	41°	329°	2.568	.285	(N=9)

Table 2. - Continued

	R	T	N	θ	φ	ε_i^2	ε_i^2/N	
$\hat{e}_{III}^{max\ 1}$	-.551	.821	.147	147°	10°	1.271	.141	
$\hat{e}_{I}^{max\ 2}$	.268	-.269	.925	74°	106°	6.971	.581	
$\hat{e}_{II}^{max\ 2}$	.245	.948	.205	76°	12°	2.985	.259	(N=12)
$\hat{e}_{III}^{max\ 2}$	.932	-.172	-.320	21°	242°	2.044	.170	
$\hat{e}_{I}^{max\ 3}$	.469	.168	.867	62°	79°	2.479	.496	
$\hat{e}_{II}^{max\ 3}$	.191	.939	-.285	79°	343°	1.387	.277	(N=5)
$\hat{e}_{III}^{max\ 3}$	.863	-.299	-.408	30°	234°	1.134	.267	

A comparison of these results with those for $\Delta\underline{B}$ across the discontinuities indicates two facts. First, the φ angles for the most favored eigenvectors are very nearly the same so that the orientations in the TN plane are very similar for all three groups. Second, there is a distinct difference in θ. The main fluctuations due to the Alfven waves are 10-20° closer to the TN plane than is the case for the discontinuities for all three groups. Thus on the whole, the Alfven wave fluctuations tend to lie closer to the N-axis by a significant, non-negligible amount, thus separating the planes of polarization of Alfven waves and rotational discontinuities.

3. Tangential Discontinuities and Rotational Discontinuities

Besides the rotational discontinuities discussed here, a number of tangential discontinuities were also found during the first 40 days of the flight. These tangential discontinuities were identified by using the steady-state criterion and the condition dealing with standard deviations in $\underline{B}$ previously mentioned here for events in which there was a 20% or more change in density between successive points. In addition the pressure balance equation and the condition that $\Delta\underline{V} \cdot \hat{n} = 0$ where $\hat{n} = \underline{B}_1 \times \underline{B}_2 / |\underline{B}_1 \times \underline{B}_2|$ were checked for validity across the tangential discontinuities. In all, 35 events were identified (Turner, 1971).

There were several qualitative and quantitative differences between the tangential and rotational discontinuities. The tangential discontinuities occurred throughout the 40 days in no particular pattern and during both high and low speed streams whereas the rotational discontinuities occurred during only high speed streams and in the three groups. In addition, the tangential discontinuities occurred with wide ranges in $|\underline{B}|$ and n as opposed to the rotational discontinuities which occurred during times of high $|\underline{B}|$ and low n.

The tangential discontinuity planes showed a strong preference in orientation as determined by the normal $\hat{n}$. The preferential direction of $\underline{B}_1 \times \underline{B}_2$ as determined by the matrix technique for tangential and rotational discontinuities is

presented in Table 3 and it can be noted immediately that $\underline{B}_1 \times \underline{B}_2$ is quite different for the two types of discontinuities.

Table 3. - Most Favored Direction of $\underline{B}_1 \times \underline{B}_2$ for Tangential and Rotational Discontinuities

	R	T	N	θ	φ	ε_i^2	
$\hat{e}_I$	.820	.552	-.150	35°	335°	18.029	
$\hat{e}_{II}$	.018	.237	.971	89°	76°	10.162	(Tangential Discont)
$\hat{e}_{III}$	-.572	.880	-.184	145°	348°	6.180°	
$\hat{e}_I$	.516	.645	-.563	59°	319°	6.287	
$\hat{e}_{II}$	-.343	.758	.554	150°	36°	4.025	(Group I)
$\hat{e}_{III}$	.785	-.093	.613	38°	99°	2.688	
$\hat{e}_I$	.443	.796	-.460	64°	329°	8.123	
$\hat{e}_{II}$	-.260	.601	.756	165°	52°	5.258	(Group II)
$\hat{e}_{III}$	.858	-.215	.466	31°	115°	2.619	
$\hat{e}_I$	.745	.057	-.665	42°	275°	4.874	
$\hat{e}_{II}$	.207	.927	.312	78°	19°	1.775	(Group III)
$\hat{e}_{III}$	.634	-.370	.679	51°	119°	0.351	

Thus tangential and rotational discontinuities differ markedly in the orientation of $\underline{B}_1 \times \underline{B}_2$. In addition, there are also sharp differences in the state of the solar wind and interplanetary magnetic field when they occur as well as differences in their patterns of occurrence in time.

4. A Comparison of Fast and Slow Solar Wind Streams

Since both Alfven waves and rotational discontinuities seem to depend heavily on the existence of fast solar wind streams for their existence, a brief comparison of these streams with slow streams may be in order. In this case, a stream is taken to be plasma flowing past the spacecraft over a four or five day interval with bulk velocities which are consistently high (i.e. $\gtrsim$ 390 km/sec) or consistently low (i.e. $\lesssim$350 km/sec). In this section, all days which seemed to be in transition regions between fast and slow streams were not considered.

The average radial velocity during the fast streams was 438 km/sec as compared with 320 km/sec for the slow streams. Figures 3 and 4 indicate two qualitative differences in values of $|\underline{B}|$ and n during fast and slow streams. The averages of $|\underline{B}|$ and n were 7.0γ and 4.9 particles/cc respectively during fast streams and 4.6γ and 12.0 particles/cc for slow streams. One clear result of this is that the Alfven speed would tend to be much higher in the fast streams. In addition to differences in field strength during fast and slow streams, there also

appeared to be a structural difference. The field imbedded in the slow streams has a positive, i.e. radially outward, polarity 35% of the time based on hourly averages, while this figure is only 19% for the fast streams. For both types of streams, when there was a period of outward polarity it either persisted for several hours or only appeared briefly during times heavily dominated by inward polarity. At least on the scale of an hour, there were few if any cases in which the polarity changed back and forth for several hours.

There were marked differences in the velocity and magnetic field fluctuations during fast and slow streams. A comparison of the flows can be seen from Figure 9 in which the number of times per day $|\Delta \underline{V}| \geq$ 25 km/sec occurs between consecutive points. From Figures 2 and 9 it can be easily seen that when the bulk speed is high there seem to be several of these changes each day while for lower velocities the number is at or near zero. It is very possible that at least some of these abrupt velocity changes could have been identified as rotational discontinuities if less stringent conditions for acceptance had been imposed. This is especially true for the steady-state condition. During all fast streams studied (except for one), the R direction was strongly favored as the most likely direction for fluctuations in $\underline{V}$. In the one exception the R and N directions seemed to be on equal footing as the most favored. For the slow streams the situation is reversed, that is, with the exception of one stream, fluctuations in the R direction were definitely subordinate in comparison with fluctuations in the TN plane. In the one exception, the most likely

direction of fluctuation was approximately mid-way between the R and N axes. Thus from Figure 9 and the above mentioned findings, it is clear that sudden velocity changes in general and V_R changes in particular are much more likely in fast streams. This allows for the possible "collision" of relatively higher and lower speed plasma within the fast stream.

The differences between the magnetic field fluctuations in the fast and slow streams are not quite so large. In both cases the N-direction played an important role in the fluctuations. For the fast streams, the N direction was usually strongly favored as a likely direction for fluctuations, while, during slow streams the most likely direction for fluctuations was in general not as well defined as the most likely direction was for fast streams. In addition, the most likely direction usually had the T and N directions making equal or nearly equal contributions.

The purpose of this section of the discussion was to point out some of the differences between fast and slow streams. It would seem that some or all of these differences are fundamental to the occurrence of rotational discontinuities since they tend to be associated with the fast streams. The rotational discontinuities indeed seemed coupled to the existence of smooth Alfven waves along with a significant difference in bulk speeds.

Conclusions

1. Rotational discontinuities exist in the solar wind and are imbedded in a sea of smoother Alfven waves in high velocity plasma streams.

2. The change in magnetic field across the rotational discontinuities tends to be 10 - 20° away from the direction favored for the fluctuations of Alfven waves.

3. The tangential discontinuity normal tends to be oriented differently from that of the rotational discontinuities.

4. There are significant differences between fast and slow streams. Some of these differences such as velocity fluctuations, the magnetic field magnitude, and the number density probably are significantly correlated with the occurrence of rotational discontinuities.

REFERENCES

Belcher, J.W. and L. Davis, Large amplitude Alfven waves in the waves in the interplanetary medium: Mariner 5, J. Geophys. Res., 74, 2302, 1969.

Belcher, J.W. and L. Davis, Anisotropy in the microscale fluctuations of the interplanetary magnetic field, EOS, 51, 413, 1970.

Colburn, D.S. and C.P. Sonett, Discontinuities in the solar wind, Space Sci. Rev., 5, 439, 1966.

Coleman, P.J., Wavelike phenomena in the interplanetary plasma: Mariner 2, Planetary Space Sci., 15, 953, 1967.

Connor, B.V., Space magnetics: Mariner 5 magnetometer experiment, IEEE Trans. Magnetics, MAG-4, 391, 1968.

Lazarus, A.J., H.S. Bridge, J.M. Davis, and C.W. Snyder, Initial results from the Mariner 5 solar plasma experiment, Space Res., 7, 1296, 1967.

Turner, J.M., Tangential discontinuities in the solar wind, Center for Space Research Report CSR-P-71-59, MIT, 1971 (submitted to J. Geophys. Res., 1971)

Turner, J.M. and G.L. Siscoe, Orientations of rotational and tangential discontinuities in the solar wind, J. Geophys. Res., 76, 1816, 1971.

Unti, T.W.J. and M. Neugebauer, Alfven waves in the solar wind, Phys. of Fluids, 11, 563, 1968.

Acknowledgement

I am grateful to Dr. E.J. Smith of the Jet Propulsion Laboratory, Drs. Leverett Davis, Jr. and J.W. Belcher of the California Institute of Technology, Dr. P.J. Coleman, Jr. of the University of California at Los Angeles and Dr. D.E. Jones of Brigham Young University for providing me with the magnetic field data from Mariner 5. I would also like to thank Dr. A.J. Lazarus of the Massachusetts Institute of Technology for the Mariner 5 plasma data. I am grateful also for the fruitful discussions which I had with Professors S. Olbert, G.L. Siscoe and V.M. Vasyliunas.

This work is supported in part by the National Aeronautics and Space Administration under Contract NGL-22-009-015.

FIGURE CAPTIONS

Figure 1: Data from a typical rotational discontinuity are plotted. The positive ion number density, the magnetic field magnitude, and the RTN components of the velocity and magnetic field are shown.

Figure 2: The daily average of the radial component of the plasma velocity.

Figure 3: The daily average of the magnitude of the magnetic field.

Figure 4. The daily average of the positive ion number density.

Figure 5: The changes in the magnetic field across the rotational discontinuities in group I are plotted. The R-axis is taken as the polar axis and all changes are taken to point outward so that the polar angle θ is $0 \leq \theta \leq 90°$ and is plotted out from the center of the diagram. The angle ϕ which is in the TN plane is defined such that $\phi = 0$ is the positive T direction and $\phi = 90°$ is the positive N direction.

Figure 6: The changes in the magnetic field across the rotational discontinuities in group II are plotted. The angles in the diagram are the same as described in Figure 5.

Figure 7: The changes in the magnetic field across the rotational discontinuities in group III are plotted. The angles in the diagram are the same as described in Figure 5.

Figure 8: Changes in the hourly averages of the velocity and magnetic field from one hour to the next were normalized and the dot product of the normalized changes computed.

In this Figure is plotted the percentage of times for each day when the dot product was greater than 0.90 in absolute value.

Figure 9. The number of times each day when the velocity changed by 25 km/sec or more between consecutive data points.

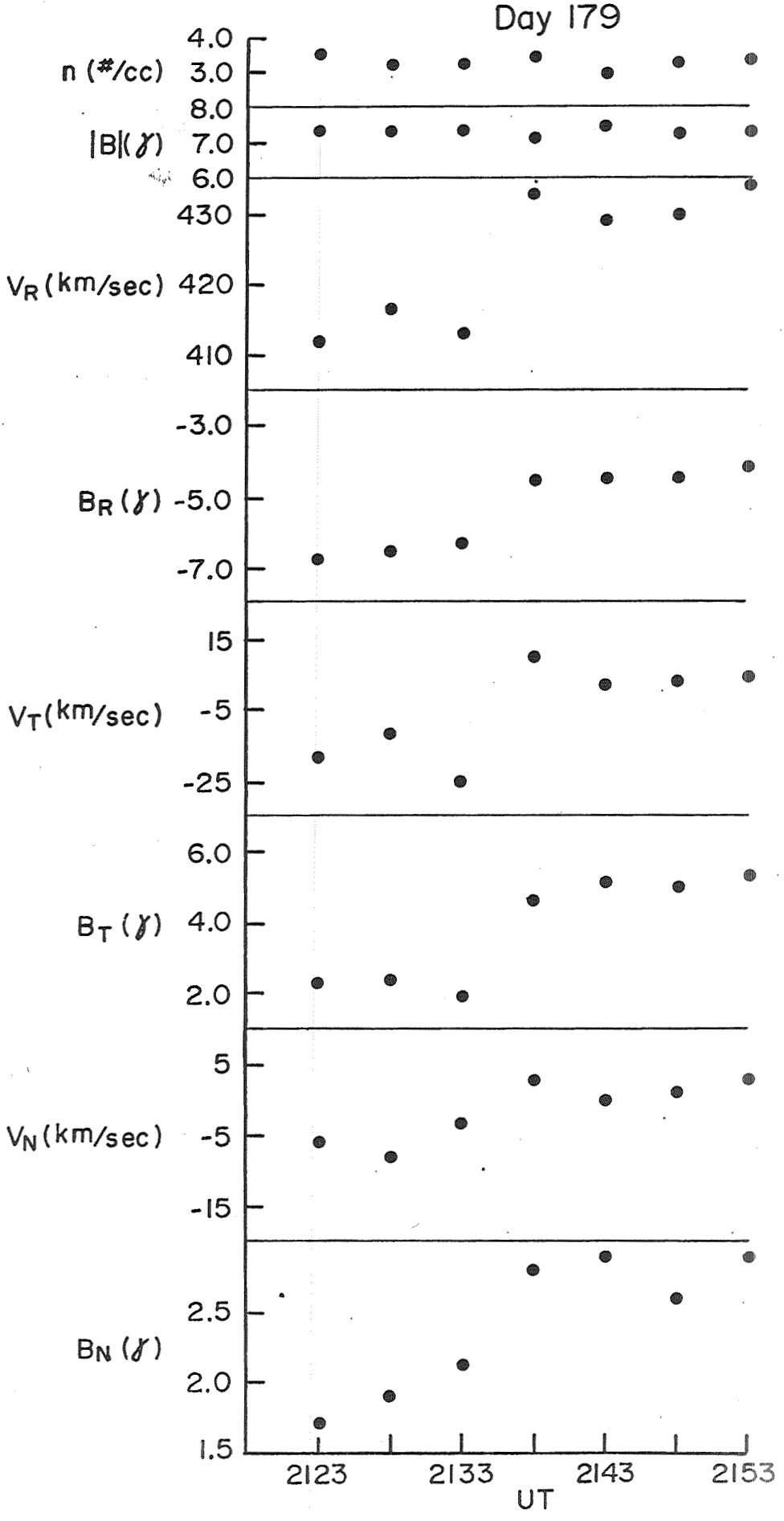
Day 179
n (#/cc)
4.0
3.0
|B|(γ)
8.0
7.0
6.0
V_R (km/sec)
430
420
410
B_R (γ)
-3.0
-5.0
-7.0
V_T (km/sec)
15
-5
-25
B_T (γ)
6.0
4.0
2.0
V_N (km/sec)
5
-5
-15
B_N (γ)
2.5
2.0
1.5
2123
2133
2143
2153
UT

Figure 1

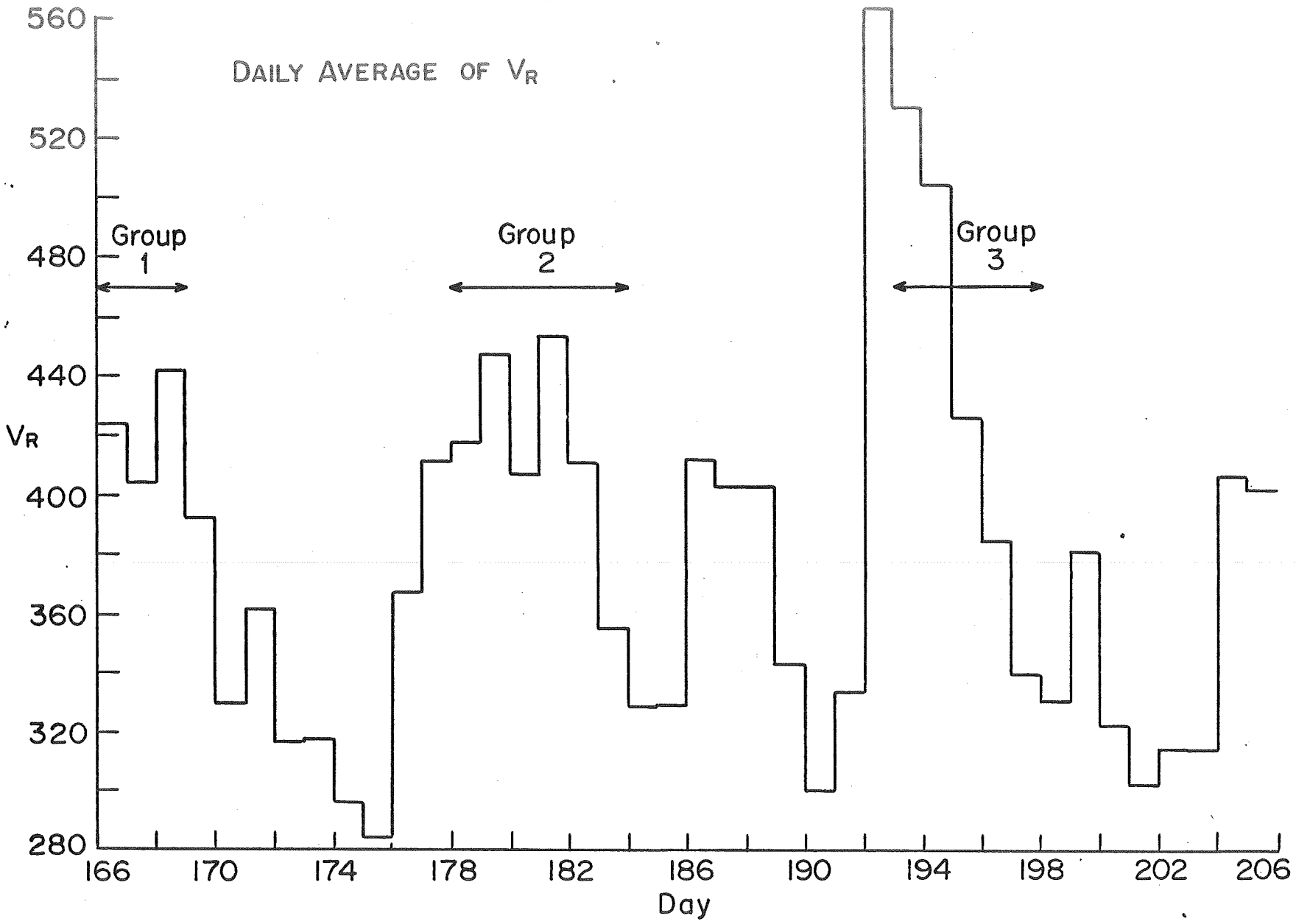
DAILY AVERAGE OF V_R
560
520
480
440
400
360
320
280
V_R
Group 1
Group 2
Group 3
166
170
174
178
182
186
190
194
198
202
206
Day

Figure 2

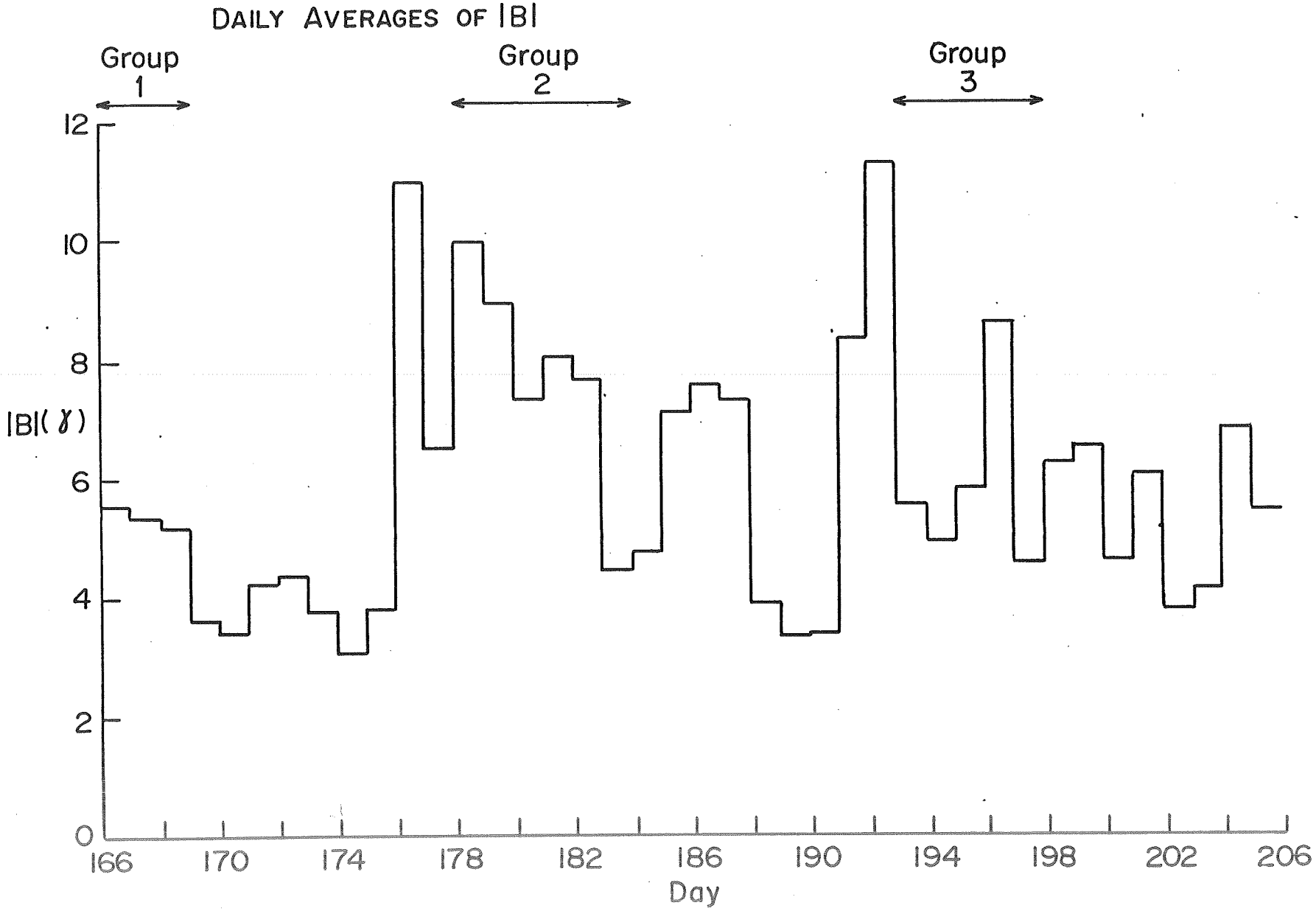
DAILY AVERAGES OF |B|
Group 1
Group 2
Group 3
12
10
8
6
4
2
0
|B|(γ)
166
170
174
178
182
186
190
194
198
202
206
Day

Figure 3

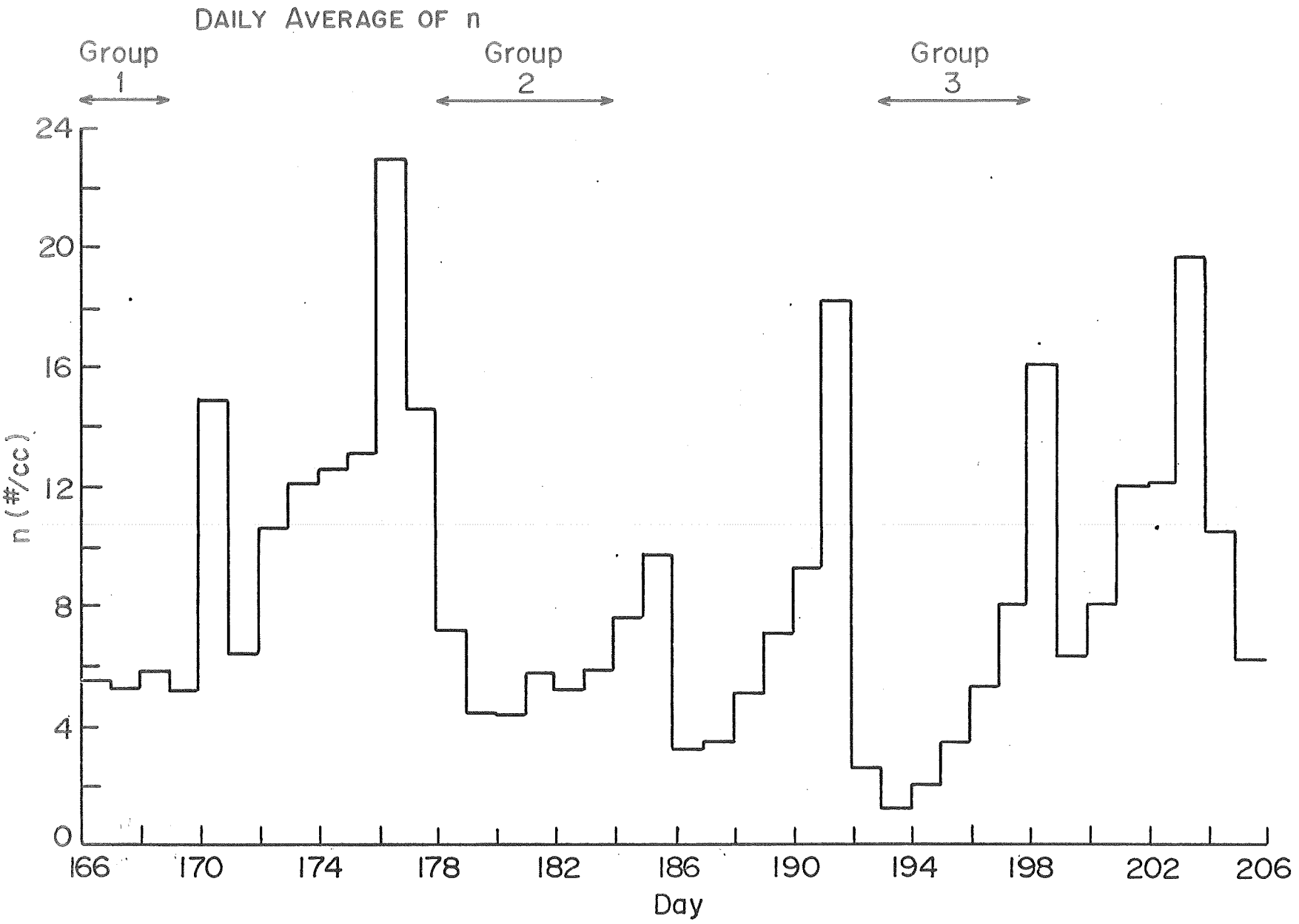
DAILY AVERAGE OF n
Group 1
Group 2
Group 3
24
20
16
12
8
4
0
n (#/cc)
166
170
174
178
182
186
190
194
198
202
206
Day

Figure 4

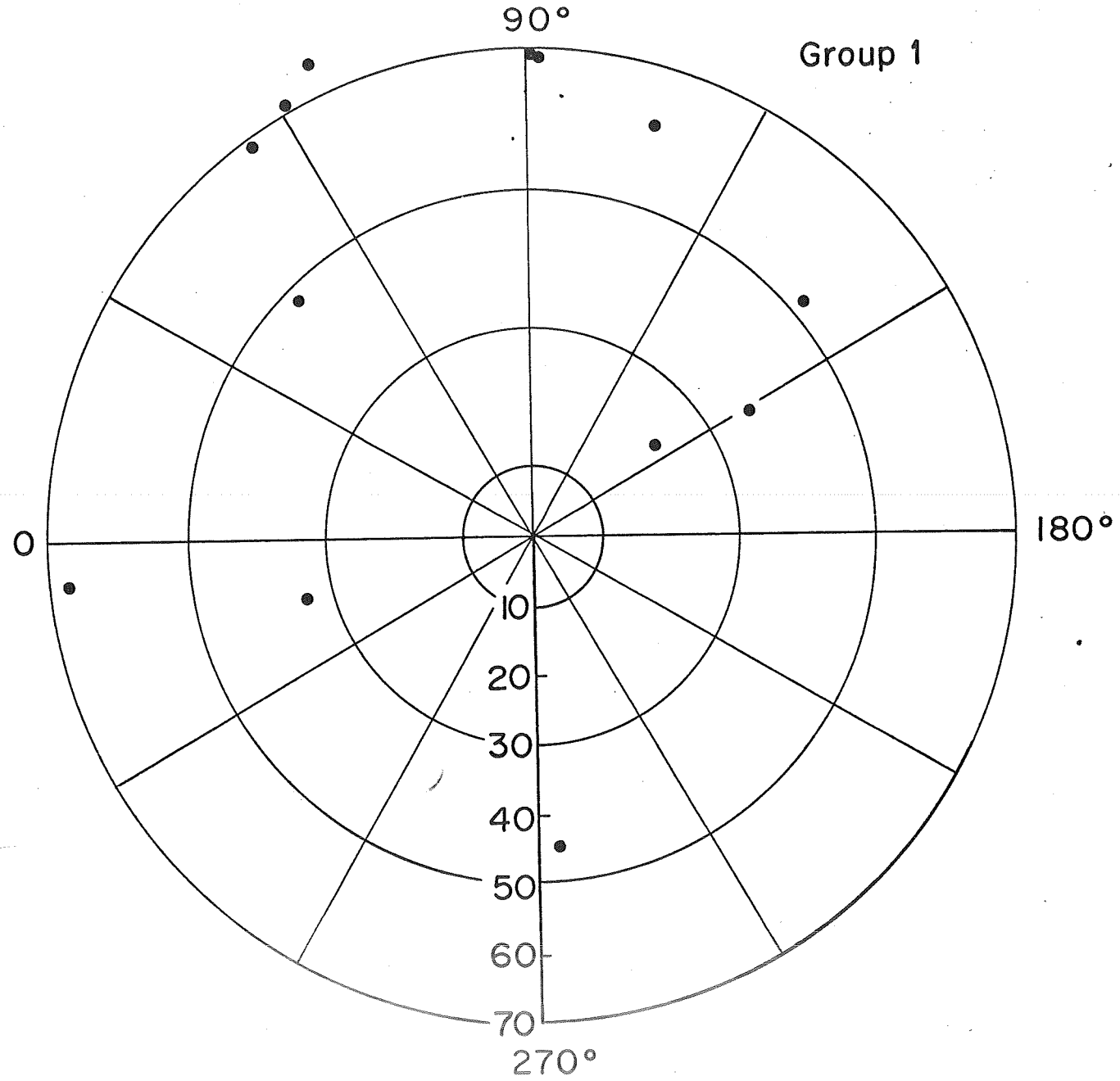

Figure 5

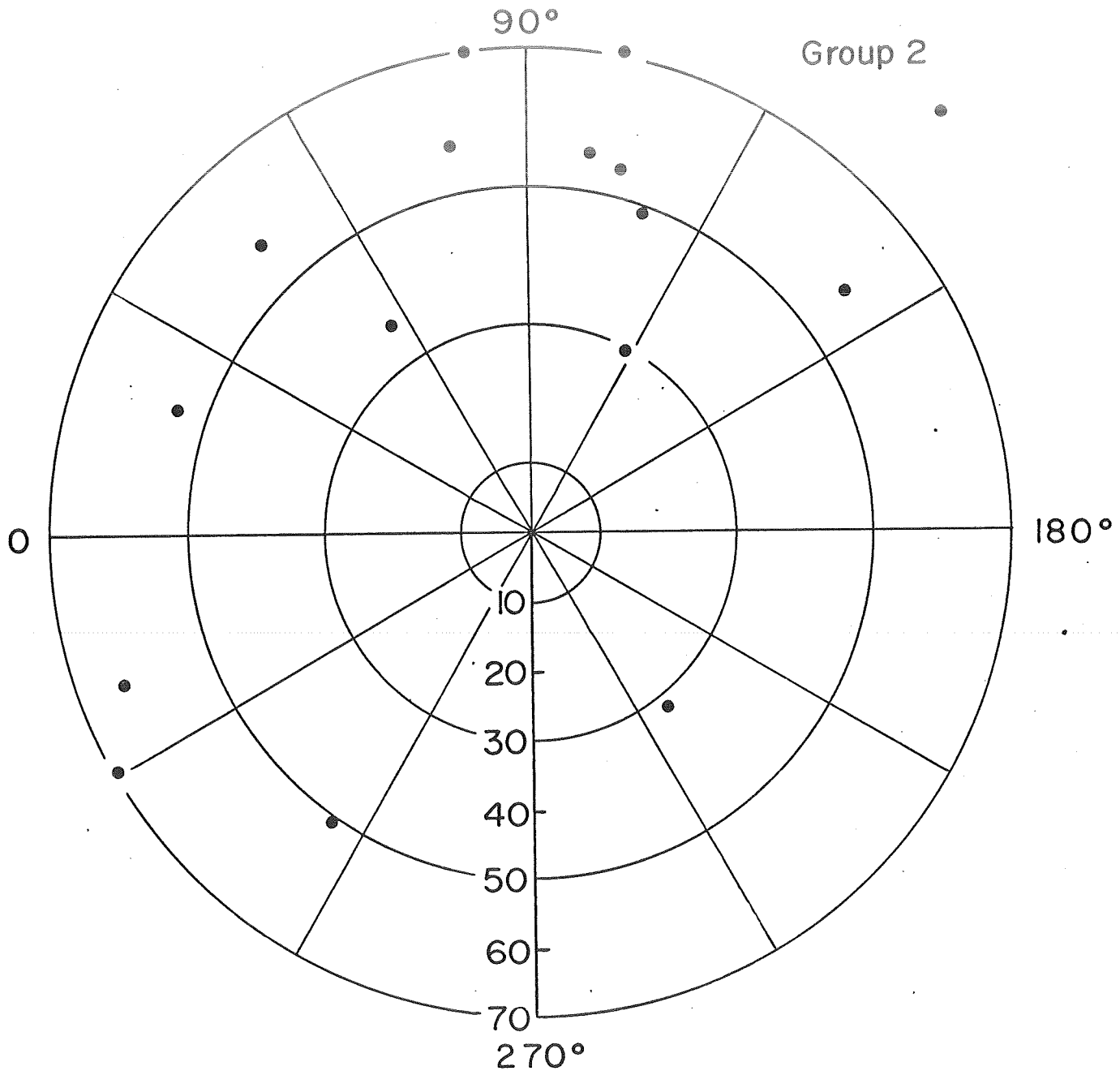

Figure 6

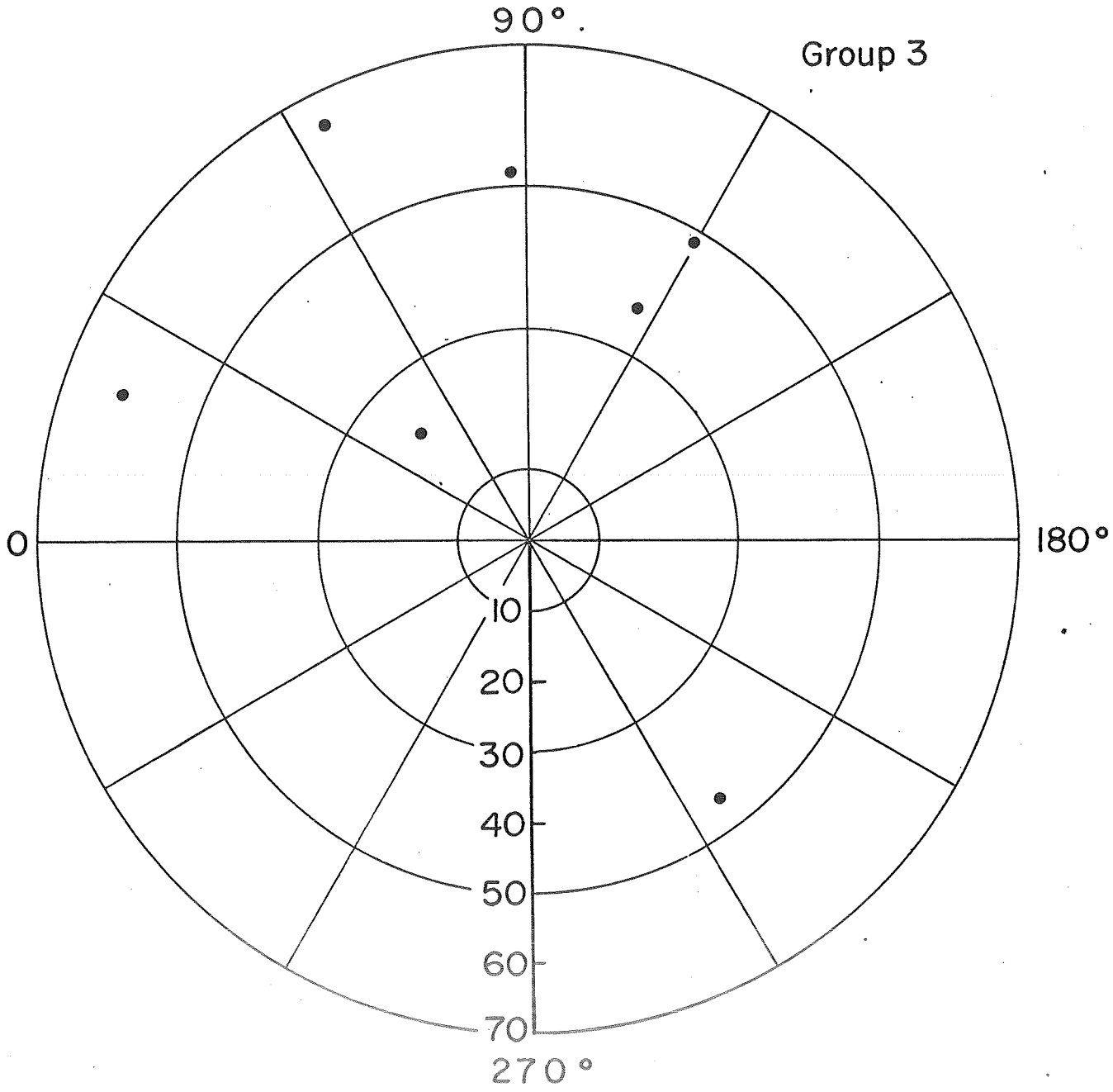

Figure 7

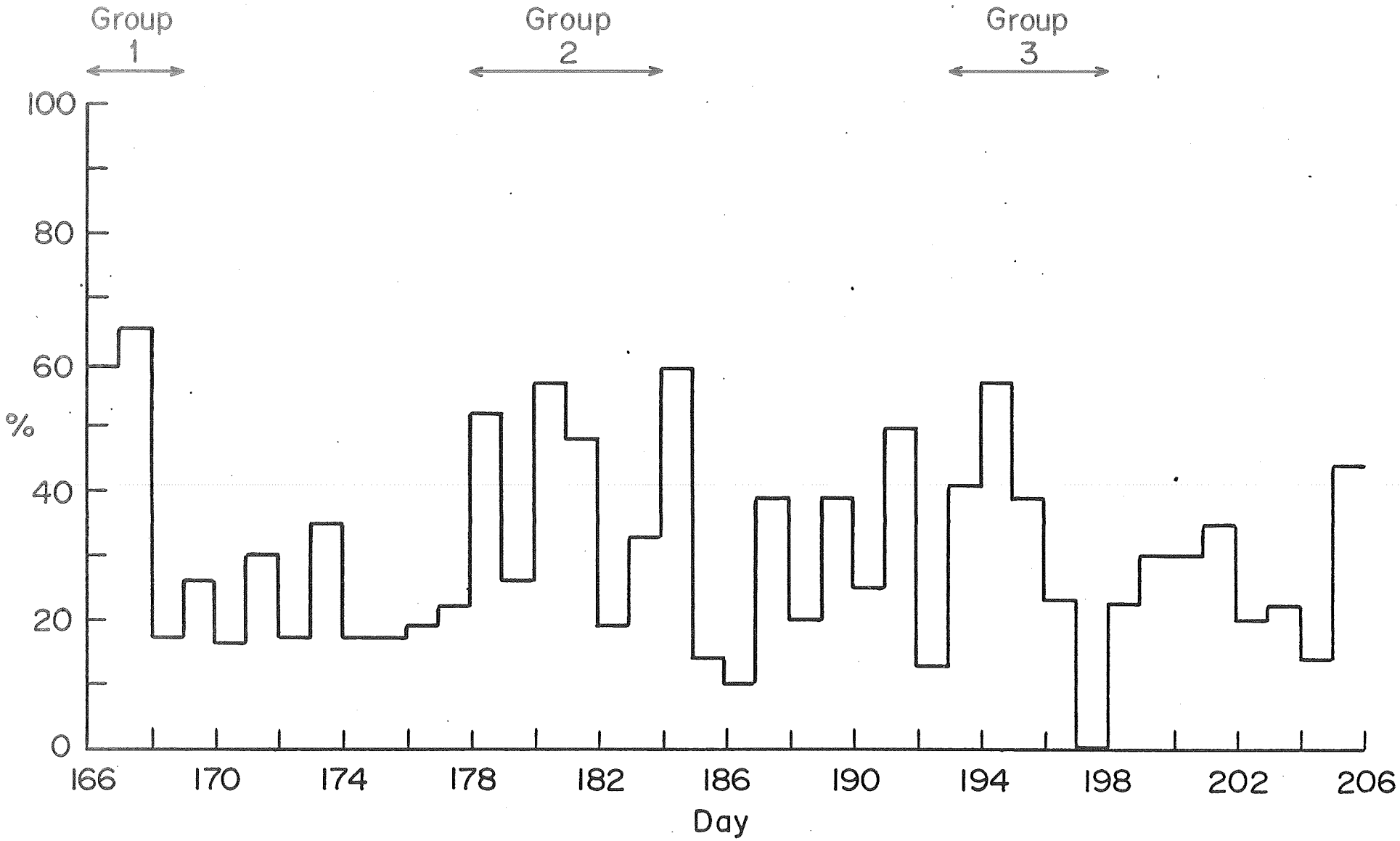
Group 1
Group 2
Group 3
100
80
60
40
20
0
%
166
170
174
178
182
186
190
194
198
202
206
Day

Figure 8

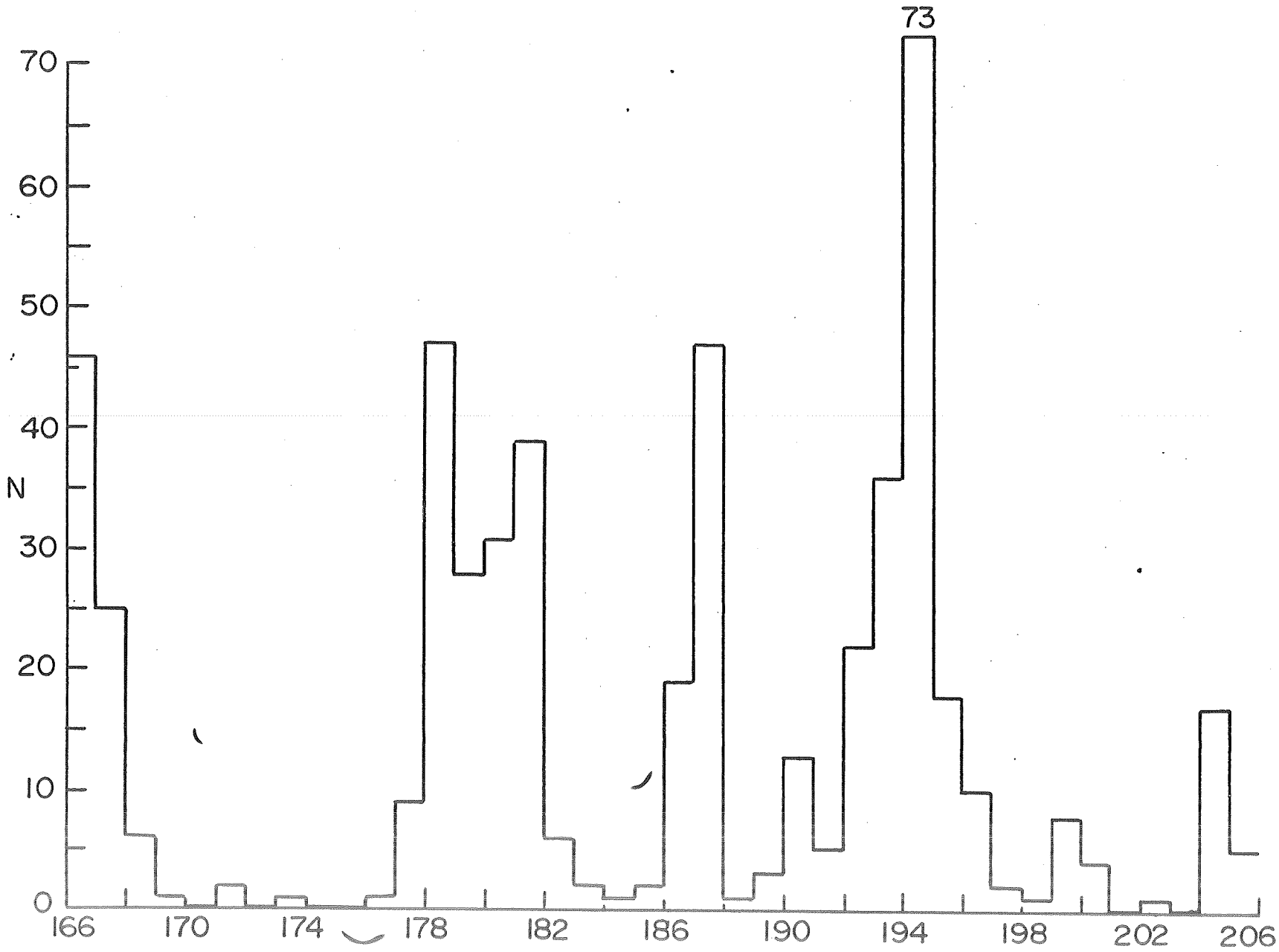
73
70
60
50
40
N
30
20
10
0
166
170
174
178
182
186
190
194
198
202
206
Day

Figure 9